Current Microbiology (2024) 81:151
https://doi.org/10.1007/s00284-024-03670-4

Biological Synthesis of Silver Nanoparticles from *Lavandula mairei* Humbert: Antibacterial and Antioxidant Activities

Soufiane EL Megdar[1] · Lahbib Fayzi[2] · Raja Elkheloui[1] · Asma Laktib[1] · Mohamed Bourouache[1] · Abdellah EL Boulani[1] · Hicham Abou Oualid[3] · Khalil Cherifi[2] · Fouad Msanda[2] · Mohamed Hassi[1] · Rachida Mimouni[1] · Fatima Hamadi[1]

Received: 27 June 2023 / Accepted: 18 March 2024 / Published online: 22 April 2024

Abstract

Hospital-acquired infections involving carbapenem-resistant *Acinetobacter baumannii (A. baumannii)* and extended spectrum beta-lactamase (ESBL)-producing Enterobacteriaceae pose significant challenges in the intensive care units. The lack of novel antimicrobial drugs amplifies the urgency to explore innovative management strategies. Nanotechnology, with its ability to generate nanoparticles possessing specific properties beneficial in drug delivery and nanomedicine, stands as a pivotal research domain. The objective of this study was to synthesize, for the first time, biologically silver nanoparticles (Ag-NPs) from *Lavandula mairei* Humbert *(L. mairei)* plant. The biosynthesized Ag-NPs were characterized by UV–visible spectral analysis, X-Ray diffraction Analysis, Fourier transform infrared spectroscopy analysis, scanning electron microscopy (SEM), and energy-dispersive X-ray spectroscopy. Subsequently, the antibacterial and antioxidant activities of Ag-NPs were assessed using the micro-dilution method, DPPH test and FRAP assay, respectively. The green-synthesized Ag-NPs exhibited high antibacterial activity against ESBL-producing multidrug-resistant (MDR) strains and against carbapenem-resistant and non-carbapenem-resistant strains of *A. baumannii*, as well as a very interesting antioxidant activity. The present study suggests that these results hold very promising for the potential application of biologically synthesized Ag-NPs from *L. mairei* (Ag-LM-NPs) in the invention of novel antibacterial and antioxidant agents.

Introduction

The extensive use of antibiotics significantly contributes to the emergence of MDR bacteria. A kind of drug resistance known as antibiotic resistance occurs when a bacterium can withstand exposure to an antibiotic [1]. Antibiotic resistance is a serious problem to human health, causing an estimated 0.7 million deaths annually worldwide [2]. Currently, due to MDRs, an alarming increase in bacterial infections has been seen. Nearly 70% of the pathogens causing hospital-acquired infections have become resistant to at least one of the most commonly prescribed drugs. Some bacterial pathogens cannot be treated with any of the approved antibiotics; instead, they may be compulsorily treated with experimental, potentially harmful medications [3]. Many bacterial strains have developed resistance to several antibiotics. Notably alarming are ESBL-producing bacteria and *A. baumannii* [4–6]. The majority of ESBL-producing bacteria belong to the Enterobacteriaceae family, which includes *Enterobacter cloacae (E. cloacae), Klebsiella pneumoniae (K. pneumonia)*, and *Escherichia coli (E. coli)* [5]. These bacteria are a growing problem due to their hydrolysis activity against third generation extended spectrum cephalosporins like ceftazidime, ceftriaxone, cefotaxime, and monobactam aztreonam, frequently used in the treatment of nosocomial infections [7]. In addition, *A. baumannii* is implicated in severe hospital-acquired infections, notably ventilator-associated pneumonia, urinary tract, central nervous system infections, and bacteremia [8, 9]. Despite clinical studies indicating the effectiveness of carbapenem, specifically imipenem, meropenem, and doripenem, against *A. baumannii*, resistance

✉ Fatima Hamadi
f.hamadi@uiz.ac.ma

[1] Laboratory of Microbial Biotechnology and Plants Protection. Biology, Department. Sciences Faculty, Ibn Zohr University, Agadir, Morocco

[2] Laboratory of Biotechnologies and Valorization of Natural Resources, Biology Department. Sciences Faculty, Ibn Zohr University, Agadir, Morocco

[3] Green Energy Park, Institut de Recherche en Energie Solaire Et Energies Nouvelles (IRESEN), Benguerir, Morocco

has developed against these agents, rendering the bacterium resistant to most antibiotics [10]. Consequently, efforts must be redirected toward the discovery of novel antibacterial agents to curb the spread of these antibiotic-resistant pathogens. Several studies have indicated that silver nanoparticles may be a potential solution to address the problem of antibiotic resistance, as their efficacy against various MDR bacteria has been reported [11, 12].

In recent years, there has been a notable surge in focus on the production of environmentally friendly metal nanoparticles within the realms of materials science and biotechnology. These nanoparticles exhibit distinctive attributes, such as shape, size, conductivity, and self-assembly, owing to their high 'surface-to-volume ratio.' Among the various metal nanoparticles, silver nanoparticles have captivated significant attention due to their versatile applications, encompassing antibacterial, antioxidant, anti-cancer, and anti-biofilm properties [11–14]. However, conventional chemical and physical techniques employed for nanoparticle production are characterized by their high costs, time-consuming procedures, and energy-intensive processes. Furthermore, the chemical reducing agents utilized in these methods raise environmental concerns. Consequently, there is a pressing need to explore alternative approaches to surmount these limitations and develop more sustainable synthesis methods for these nanoparticles.

Biological synthesis methods have been employed as alternatives to chemical and physical methods. Many investigations have affirmed that the biosynthesis of silver nanoparticles supersedes physical and chemical methods, primarily due to its environmentally friendly and cost-effective nature [15, 16]. This biological synthesis can be performed utilizing diverse biological resources, such as fungi [17], bacteria [18], and plants [19]. Among these options, the utilization of plant sources is particularly favored in this field, due to the ability to produce larger quantities of more stable nanoparticles and the decrease and simplicity of the synthesis steps [20]. The presence of bioactive components such as flavonoids, terpenoids, phenols, and alcohols in plant extracts facilitates the generation of Ag-NPs through the reduction of Ag^{+} ions to Ag^{o} [21].

Lavandula L. constitutes a genus of considerable economic importance among floral plants within the Lamiaceae family. In Morocco, this genus encompasses nine recognized subspecies and species, five of which are endemic [22]. Among these species, *L. mairei* emerges as an endemic vivacious shrub adorned with spiky purple flowers. It thrives in the arid and semi-arid Saharan bioclimates, spanning from southeastern to mountainous southwest Morocco [22]. Remarkably, to our knowledge, *L. mairei* has never been used for nanoparticle synthesis in general and silver nanoparticles specifically. Therefore, the objectives of this study are as follows: *i*) to synthesize silver nanoparticles for the first time using the aqueous extract of *L. mairei, ii)* to characterize these biological nanoparticles, and *iii)* to evaluate their antioxidant and antibacterial activity against nineteen strains.

Materials and Methods

Bacterial Strains

Seventeen MDR strains were isolated and identified by our laboratory [8]. Among these, ten strains were classified as *A. baumannii* species: comprising four non-carbapenem-resistant strains (*AB* 8, *AB* 9, *AB* 10, and *AB* 11) and six carbapenem-resistant strains (*AB* 1, *AB* 2, *AB* 3, *AB* 4, *AB* 5, and *AB* 6) that demonstrated resistance to Imipenem and Meropenem [6]. Additionally, seven strains of ESBL-producing Enterobacteriaceae were also selected, including three strains of *E. coli* (*E. coli* 1, *E. coli* 2, and *E. coli* 3), three strains of *K. pneumoniae* (*KPP* 2, *KPP* 4, and *KPP* 9), and one strain of *E. cloacae*. Moreover, reference strains (*E. coli* ATCC 25922 and *Pseudomonas aeruginosa (P. aeruginosa*) ATCC 27853) were also tested.

Plant Extracts

The aerial parts of wild *L. mairei* were collected in May 2020 from Sidi Mzal village, in the southwest region of Morocco, located in the Anti-Atlas Mountains (29°51′19.1" N, 8°54′51.6" W, elevation 1240 m). The plant species was identified by a plant biologist from the Biology Department, Sciences Faculty**,** Ibn Zohr University, Agadir, Morocco. A reference specimen (LM114) of the plant was placed in the Laboratory of Biotechnology and Valorization of Natural Resources**,** Ibn Zohr University. The shade-dried plant material was finely ground with a grinder and preserved in an airtight container at 4 °C for future use.

Preparation of Aqueous Extract of *L. Mairei*

The preparation of the aqueous plant extract was performed according to the protocol of Qais et al. [23], with some modification. Five grams of powdered aerial part of *L. mairei* were added to 100 mL of distilled water in an Erlenmeyer flask and stirred carefully. The solution was then heated to 90 °C and stirred for 30 min using a magnetic hot plate stirrer. Afterward, it was cooled to room temperature, filtered through Whatman filter paper No. 1, and then stored at − 20 °C for future use.

Biosynthesis of Silver Nanoparticles using *L. Mairei* Aqueous Extract

Prior to initiating the process, a 1-mM aqueous solution of silver nitrate ($AgNO_3$) was prepared in a dark environment to prevent photoactivation. The formation of Ag-NPs was monitored by observing color changes through spectrophotometric measurements. For the synthesis of Ag-LM-NPs, 0.5 mL of *L. mairei* aqueous extract was added to 20 mL of the 1-mM silver nitrate solution. The reaction was carried out at 37 °C for 24 h with continuous stirring to ensure thorough agitation for the bio-reduction of $AgNO_3$ by plant extract components. The reduction of silver ions to silver nanoparticles was initially detected by a color change from colorless to dark brown. Subsequently, the formed Ag-LM-NPs were centrifuged at 9500 rpm for 30 min. The resulting pellets were re-suspended in bidistilled water, re-centrifuged, and lyophilized to obtain the nanoparticles in powder form, which were stored at 4 °C for future research.

Characterization of Biosynthesized Silver Nanoparticles

UV–Visible Spectral Analysis

In order to determine the capacity of *L. mairei's* aqueous extract in reducing silver ions from silver nitrate to silver nanoparticles, a preliminary characterization of Ag-LM-NPs was performed using a UV–visible spectrophotometer (JENWAY). The absorbance spectra of the reaction mixture, $AgNO_3$, and *L. mairei* aqueous extract were recorded by continuous scanning between 300 and 800 nm.

X-Ray Diffraction Analysis (XRD)

The synthesized Ag-LM-NPs were characterized as a powder using an X-ray diffractometer Bruker D8 Advance Twin (at the Faculty of Sciences Agadir, Morocco), with Cu Kα radiation ($\lambda = 1{:}5404$ Å) in the range of 2θ from 10 to 100°.

Using the Debye–Scherrer equation [21], which is defined in Eq. (1), the average crystallite size (D, nm) of the Ag-NPs is estimated.

$$D = k\lambda / \beta \cos\theta \quad (1)$$

where D is the crystallite size, k denotes the shape factor, λ represents the wavelength of the XRD, β is the half-width of the peak, and θ represents the angle of diffraction.

Scanning Electron Microscopy (SEM)

Scanning electron microscopy (SEM) was employed to explore and examine the morphology and size of the samples. For SEM analysis, the surface of the elements needed to be electrically conductive. To enhance conductivity and image precision, a powdered sample of Ag-LM-NPs was deposited on a carbon-coated plate and subsequently coated with gold using a sputtering device. The SEM analysis was conducted using a scanning electron microscopy (JEOL JSM IT100).

Energy-Dispersive X-ray Spectroscopy (EDS)

Energy-dispersive X-ray spectroscopy (EDS) was used to confirm the presence of elementary silver in Ag-LM-NPs. The analysis involved depositing the fine powder of the nanoparticles on a microscope slide and using a scanning electron microscopy JSM-IT100 equipped with a JEOL-made EDS for examination.

Fourier Transform Infrared Spectroscopy Analysis (FTIR)

The presence of functional groups in the extract of the aerial part of *L. mairei* used in the biosynthesis of Ag-LM-NPs was confirmed using an IR Affinity-1S FTIR spectrophotometer (Shimadzu). The analysis was conducted over a wavelength range of 400–4000 cm^{-1}.

Biotechnological Application of Silver Nanoparticles

Evaluation of the Antimicrobial Activity by the Minimum Inhibitory Concentration (MIC) and Minimum Bactericidal Concentration (MBC)

The MIC was determined in Muller Hinton Broth (MHB) by the micro-dilution method as described by previous researchers [6], with slight modifications. To obtain a bacterial suspension of approximately 10^6 CFU/mL, a fresh overnight culture was prepared and diluted in MHB. The biosynthesized silver nanoparticles sample was diluted in 96-well microtiter plates in MHB medium, resulting in a final volume of 100 µL. Subsequently, 100 µL of the bacterial suspension was added to obtain a final concentration range of Ag-LM-NPs from 5000 to 78 µg/mL. Following this, the plates were incubated for 24 h at 37 °C with continuous agitation. Negative and positive controls consisted of MHB medium and bacterial suspension, respectively. After 24 h, TTC (2, 3, 5-triphenyl tetrazolium chloride, Sigma), a growth indicator, was added to each well to assess bacterial growth inhibition. Bacterial growth was visually observed as the uncolored TTC turned to pink-red formazan in the presence of bacteria. The MIC was determined as the lowest concentration at which no observable growth occurred.

Following MIC determination, 10 µL from wells without any color change were streaked onto Tryptic Soy agar (TSA) plates and incubated at 37 °C for 24 h. The

MBC was determined as the lowest concentration at which the viability of the inoculum was decreased to 99.9% or 100%.

Antioxidant Activity

2, 2-Diphenyl-1-Picryl-Hydrazyl-Hydrate (DPPH) Test The antioxidant activity of the biosynthesized nanoparticles was tested using the DPPH radical scavenging assay as reported by [24], with some modifications. Initially, a fresh solution of 60-µM DPPH was prepared in methanol and kept light protected. Subsequently, one milliliter of this solution was added to 25 µL of Ag-NPs samples (ranging from 250 to 1.95 µg/mL). The mixture was vortexed and incubated at room temperature in the dark for 30 min. After incubation, the reduction of DPPH was quantified using spectrophotometry at 517 nm. Ascorbic acid was employed as a positive control, and methanol as a negative control. All experiments were repeated in triplicate and the results were presented as mean ± SD. The percentages of scavenging activity are calculated using the equation given by [25].

$$Inhibition\,\% = (A_{control} - A_{sample})/A_{control})\,x\,100$$

The IC50 representing the concentration of the antioxidant sample required to scavenge 50% of the DPPH radical was calculated by plotting percent inhibitions against sample concentrations. The IC_{50} of the Ag-NPs sample and ascorbic acid were compared to assess their scavenging abilities. A lower IC_{50} value indicates highest antioxidant activity of the examined samples.

Ferric Reducing Antioxidant Power (FRAP) Assay The reducing power of silver nanoparticles synthesized from *L. mairei* extract was assessed following the method described by [26], with slight modifications. Briefly, 415 µL of phosphate buffer (0.2 M, pH 6.6) and 415 µL of potassium ferricyanide ($K_3Fe(CN)_6$) (1%) were mixed with 166 µL of silver nanoparticles at various concentrations (ranging from 250 to 1.95 µg/mL). The reaction mixture was then incubated in a water bath at 50 °C for 30 min. Then, 415 µL of trichloroacetic acid (1%) was added to stop the reaction and centrifuged at 2000 rpm for 10 min. Finally, 400 µL of the supernatant were mixed with 400 µL of distilled water and 80 µL of 1% ferric chloride (FeCl3). A blank solution containing all reactants without silver nanoparticles was prepared. An increase in absorbance indicates an enhancement in reducing power. The sample concentration (IC_{50}) at which the absorbance reached 0.5 was determined by plotting the absorbance at 700 nm against the corresponding silver nanoparticles concentration.

Statistical Analysis

All experiments were performed in triplicate, and the obtained data were subjected to statistical analysis using analysis of variance (ANOVA) with the use of Statistica StatSoft version 6. P values less than 0.05 were considered significant.

Nucleotide Sequence Accession Numbers

The DNA sequences of *A. baumannii* strains used in this study have been deposited in the GenBank database at the National Center for Biotechnology Information (NCBI). The accession numbers and their corresponding strains are as follows: *AB* 1 (OM338089), *AB* 2 (OM362943), *AB* 3 (OM339144), *AB* 4 (OM388305), *AB* 5 (OM338088), *AB* 6 (OM338972), *AB* 8 (OM387219), *AB* 9 (OM337870), *AB* 10 (OM388566), and *AB* 11 (OM388301).

Results

Visual Observation

A color change in the mixture was observed, when the $AgNO_3$ was added to *L. mairei* aqueous extract (Fig. 1a). This result indicates the biosynthesis of Ag-NPs after 24 h of incubation.

UV–Visible Spectral Analysis

In order to confirm the formation of silver nanoparticles, UV–visible spectrophotometry was employed to analyze the spectral range of 300–800 nm. This analytical technique is frequently employed for metallic nanoparticles characterization due to the surface plasmon resonance (SPR) phenomenon. The absorption spectrum obtained showed the presence of a maximum absorption peak at 440 nm (Fig. 1b), providing strong evidence for the presence of Ag-LM-NPs.

X-Ray Diffraction Analysis

Further characterization of the biosynthesized Ag-LM-NPs was conducted through X-ray diffraction analysis, as illustrated in Fig. 1c. According to the XRD data, silver exhibited a cubic crystal structure at 2θ angles, with discernible peaks at 111, 200, 220, and 311°. The values of these peaks were found to be 38.21°, 44.29°, 64.55°, and 77.44°, respectively. The average crystal size of the

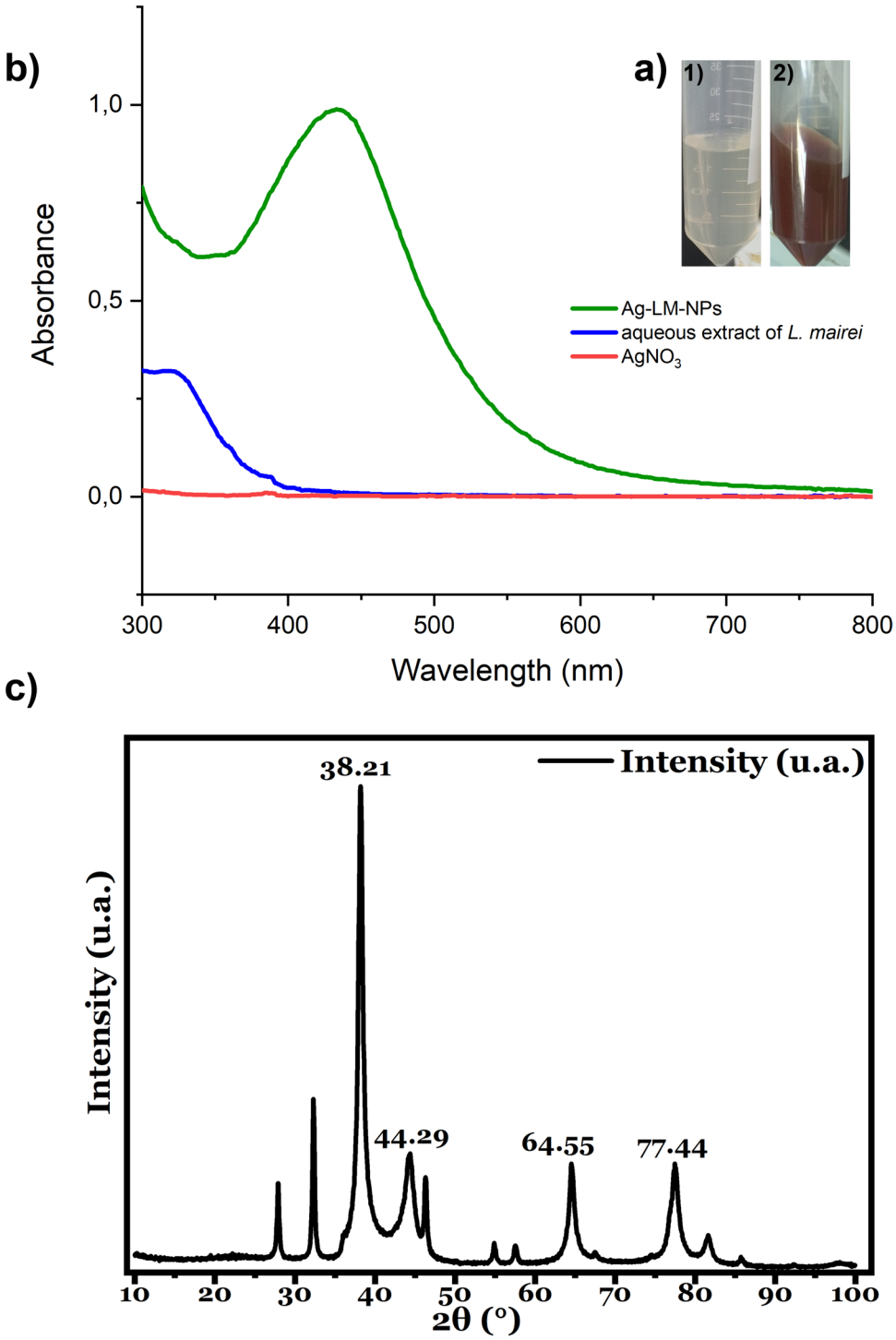

Fig. 1 **a** Visual observation of the synthesis of biological silver nanoparticles using *L. mairei*. **(1)** The initial stage (time zero) illustrates the colorless solution before synthesis, while **(2)** after 24 h shows the color change to a deep brown, indicating nanoparticle synthesis. **b** UV–visible absorption spectrum of the biological silver nanoparticles, highlighting the characteristic absorption peak of silver at 440 nm. **c** XRD pattern of the synthesized silver nanoparticles, revealing prominent peaks at 38.21°, 44.29°, 64.55°, and 77.44°, providing valuable insights into their crystalline structure

biosynthesized Ag-NPs was determined according to Eq. (1), which was 7.72 ± 1.26 nm.

Scanning Electron Microscopy

The morphological structure of the Ag-NPs synthesized from *L. mairei* extract was determined using SEM as illustrated in Fig. 2a. The SEM images showed the presence of nanoparticles with a spherical form. Although some agglomeration was observed, it was attributed to the interactions between these nanoparticles. Notably, the distribution of the synthesized silver nanoparticles appeared uniform, providing further evidence of the formation of nanosized crystallites. Additionally, the average size of these nanoparticles was estimated to be 40–70 nm, with an average size distribution of 58 nm (Fig. 2b).

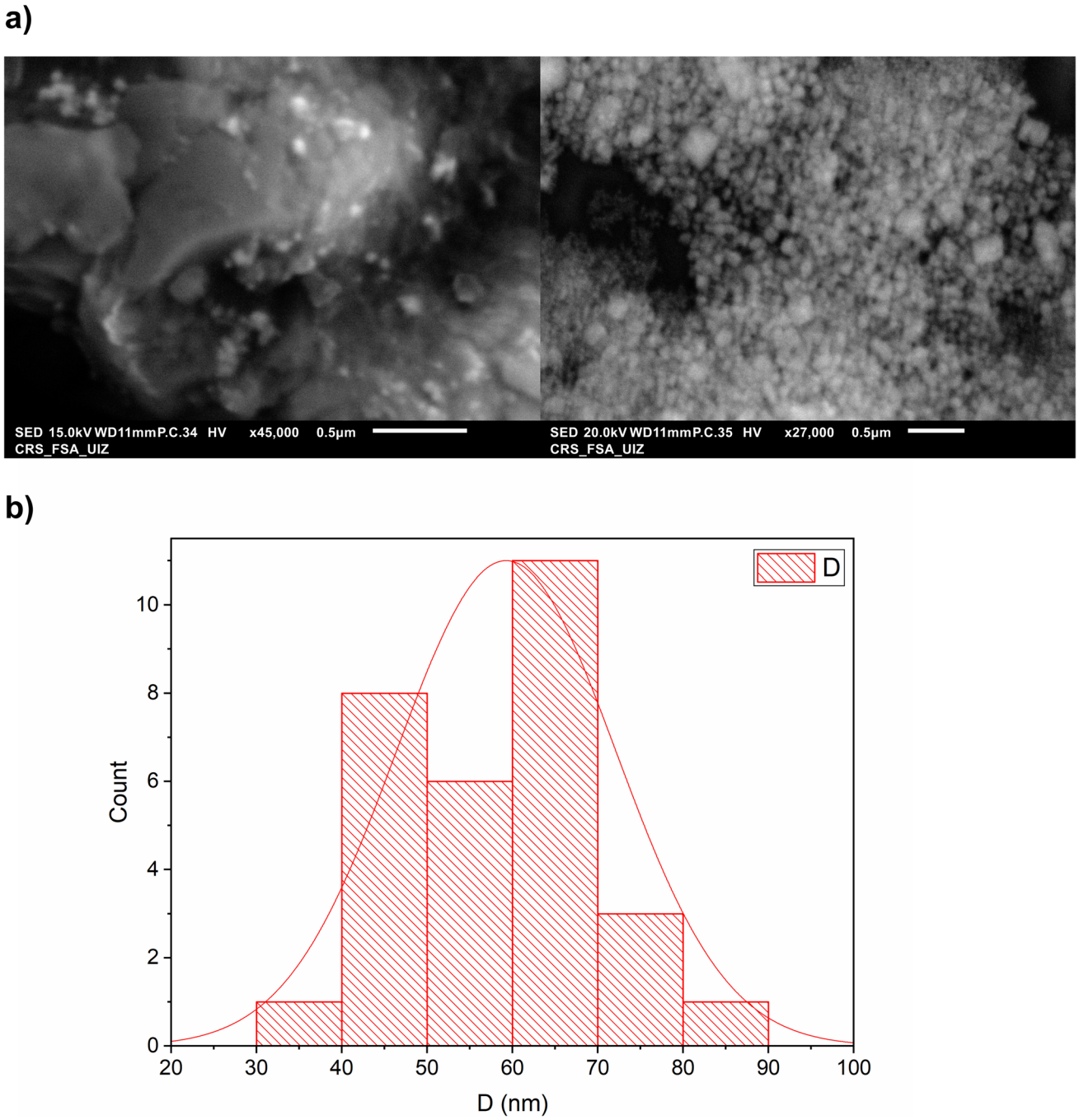

Fig. 2 **a** Scanning electron microscope images of spherical silver nanoparticles produced using the aqueous extract of *L. mairei*, giving a visual representation of their morphology. **b** Particle size distribution indicating a size between 40 and 70 nm with an average size of 58 nm, giving an insight into the homogeneity of nanoparticle size

Energy-Dispersive X-ray Spectroscopy

The results of energy-dispersive spectroscopy analysis confirm the presence of Ag-NPs produced from *L. mairei*. The analysis revealed that silver (Ag) constituted the major component of the sample, comprising 93.88% of the elemental composition. Other elements detected in lower quantities included chlorine, carbon, and oxygen (Table 1). Typically, metallic Ag-NPs display a strong optical absorption peak at 3 keV indicating the dominance of silver concentration in the elemental composition (Fig. 3).

Table 1 Percentage by weight of metallic elements present in Ag-NPs synthesized from *L. mairei* extract

Element Line	Mass%	Atom%
C K	2.34	16.20
O K	0.93	4.83
Cl K	2.85	6.67
Ag L	**93.88**	**72.30**
Total	100	100

The bolding of the mass percentage (Mass%) and atomic percentage (Atom%) values for silver (Ag L) highlights its significant importance and high purity in the composition of silver nanoparticles synthesized from *L. mairei* extract. The highlighting of the predominance of silver in the chemical composition of the sample confirms the success of the synthesis of silver nanoparticles

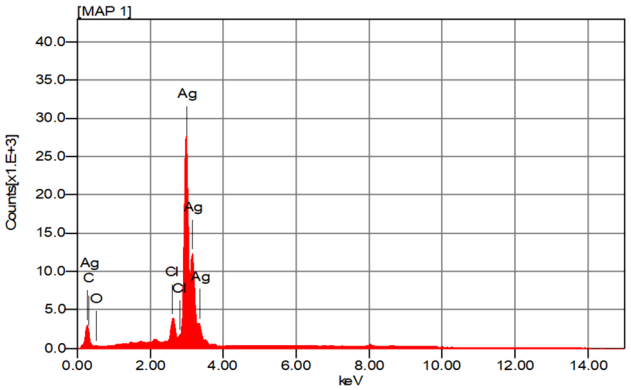

Fig. 3 EDS spectra of silver nanoparticles produced by the aqueous extract of *L. mairei*, providing elemental analysis and confirming the presence of silver in the synthesized nanoparticles

Fourier Transform Infrared Spectroscopy Analysis (FTIR)

FTIR analysis was conducted to gain insights into the potential biomolecules derived from *L. mairei* that contribute to the synthesis of silver nanoparticles. Analysis of the FTIR spectra of biosynthesized Ag-NPs reveals two strong peaks at 3415 cm^{-1} and 1651 cm^{-1} (Fig. 4).

Antibacterial Activity of Ag-NPs Against MDR Bacterial Pathogens

The MICs of biosynthesized Ag-NPs against different strains of *A. baumannii* and ESBL-producing Enterobacteriaceae species were determined using the broth micro-dilution method.

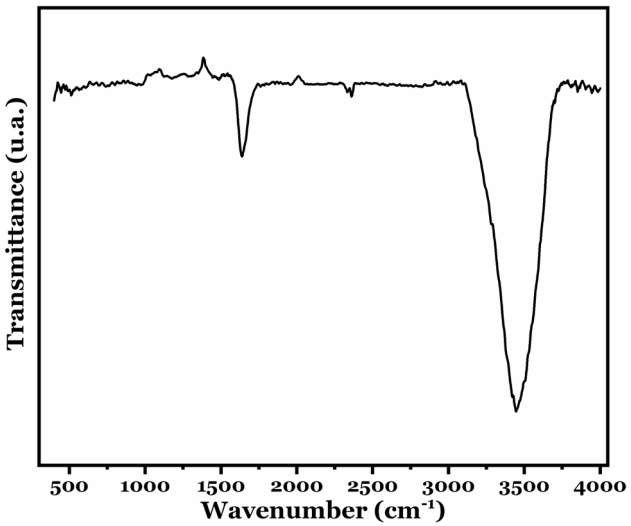

Fig. 4 FTIR spectra of biosynthesized silver nanoparticles using *L. mairei* extract, revealing characteristic peaks at 3415 cm^{-1} and 1651 cm^{-1}, indicative of functional groups involved in the nanoparticle synthesis process

Table 2 MIC and MBC of Ag- LM-NPs against carbapenem-resistant and non-carbapenem-resistant strains of *A. baumannii*

Pathogens		Ag-LM-NPs	
		MIC (µg/mL)	MBC (µg/mL)
Carbapenem-resistant strains	***AB* 1**	312 ± 0,00	312 ± 0,00
	***AB* 2**	156 ± 0,00	625 ± 0,00
	***AB* 3**	156 ± 0,00	156 ± 0,00
	***AB* 4**	312 ± 0,00	1250 ± 0,00
	***AB* 5**	156 ± 0,00	312 ± 0,00
	***AB* 6**	78 ± 0,00	625 ± 0,00
Non-Carbapenem-resistant strains	***AB* 8**	78 ± 0,00	312 ± 0,00
	***AB* 9**	312 ± 0,00	625 ± 0,00
	***AB* 10**	156 ± 0,00	625 ± 0,00
	***AB* 11**	78 ± 0,00	156 ± 0,00

The inclusion of the strain names in bold facilitates the identification and differentiation of bacterial strains. The susceptibility patterns of both carbapenem-resistant and non-carbapenem-resistant strains of *A. baumannii* to Ag-LM-NPs, as demonstrated by their MIC and MBC values

Ag-LM-NPs exhibited MICs ranging from 78 ± 0.00 to 312 ± 0.00 µg/mL and MBCs between 156 and 625 ± 0.00 µg/mL against various strains of *A. baumannii,* including carbapenem-resistant and non-carbapenem-resistant strains (Table 2). The results showed that non-carbapenem-resistant strains (*AB* 8 and *AB* 11) exhibited high sensitivity to silver nanoparticles, with MICs of 78 ± 0.00 µg/mL. This suggests that silver nanoparticles can effectively inhibit the growth of non-carbapenem-resistant *A. baumannii* strains at relatively low concentrations. However,

the majority of carbapenem-resistant strains (*AB* 1, *AB* 2, *AB* 3, *AB* 4, and *AB* 5) showed higher MICs of 156 to 312 ± 0.00 µg/mL, indicating reduced susceptibility. Overall, strains *AB* 1 and *AB* 3 exhibited an MBC equal to the MIC, while strains *AB* 5, *AB* 9, and *AB* 11 displayed an MBC twice that of the MIC. For strains *AB* 2, *AB* 4, *AB* 8, and *AB* 10, the MBC was four times higher than the MIC, and for *AB* 6, it was eight times higher than the MIC.

The results also indicated that these phyto-synthesized Ag-NPs are more effective against all species of ESBL-producing Enterobacteriaceae as well as reference species (Table 3). MIC values ranged from 78 to 625 ± 0.00 µg/mL, with *E. coli* 3 and *E. coli* ATCC 25922 displaying the lowest MIC of 78 ± 0.00 µg/mL, followed by *E. coli* 1 and *P. aeruginosa* ATCC 27853 at 156 ± 0.00 µg/mL. *E. coli* 2, *KPP* 2, and *KPP* 4 showed MIC values of 3125 ± 0.00 µg/mL, while *KPP* 9 and *E. cloacae* exhibited MIC values of 625 ± 0.00 µg/mL. Ag-NPs effectively destroyed these bacteria at concentrations (MBC) ranging from 78 ± 0.00 to 1250 ± 0.00 µg/mL. Notably, for certain bacteria such as *E. coli* 2, *E. coli* 3, *KPP* 9, and *E. coli* ATCC 25922 displayed equivalent MBC and MIC values. Statistical analysis revealed a highly significant differences (P value < 0.001) among all the tested bacteria.

Antioxidant Activity

2, 2-Diphenyl-1-Picryl-Hydrazyl-Hydrate Test

The radical scavenging capacity of silver nanoparticles together with standard ascorbic acid was established using the IC_{50}. A lower IC_{50} value indicates a better antioxidant activity. The IC_{50} of Ag-LM-NPs and ascorbic acid are presented in Table 4. The results showed that the IC_{50} value of Ag-NPs and ascorbic acid (P value < 0.001) were 38.51 ± 0.27 and 2.34 µg/mL ± 0.05, respectively. The percentage DPPH radical scavenging activity of biologically produced Ag-NPs at various concentrations varied between 11.32 and 96.43% (Fig. 5).

Table 3 MIC and MBC of Ag- LM-NPs against ESBL-producing Enterobacteriaceae strains and reference species

Pathogens	Ag-LM-NPs	
	MIC (µg/mL)	MBC (µg/mL)
E. coli 1	156 ± 0,00	312 ± 0,00
E. coli 2	312 ± 0,00	312 ± 0,00
E. coli 3	78 ± 0,00	78 ± 0,00
KPP 2	312 ± 0,00	625 ± 0,00
KPP 4	312 ± 0,00	625 ± 0,00
KPP 9	625 ± 0,00	625 ± 0,00
E. cloacae	625 ± 0,00	1250 ± 0,00
E. coli ATCC 25922	78 ± 0,00	78 ± 0,00
P. aeruginosa ATCC 27853	156 ± 0,00	312 ± 0,00

Table 4 IC_{50} of Ag-NPs and ascorbic acid by DPPH and FRAP assay

	DPPH (µg/mL)	FRAP (µg/mL)
Ag-NPs-LM	38,51 ± 0,27	17,13 ± 0,27
Ascorbic acid	2,34 ± 0,05	1.19 ± 0,01

The DPPH scavenging activity of the produced Ag-NPs was determined by the color shift from purple to yellow following the synthesis of diphenyl picrylhydrazine.

Ferric Reducing Antioxidant Power Assay

The results presented in Table 4 highlight the remarkable antioxidant activity of Ag-NPs. The concentration of Ag-NPs demonstrating 50% inhibition or efficiency (IC_{50}) was 17.13 ± 0.27 µg/mL, a value relatively comparable to that observed for ascorbic acid, used as a standard antioxidant (IC_{50} = 1.19 ± 0,01 µg/mL) (P value < 0.001).

Discussion

In the domain of eco-friendly silver nanoparticle synthesis, various biological agents such as fungi, bacteria, plants, and algae have been utilized [18]. In this study, the *L. mairei* aqueous extract was employed for the biological synthesis of silver nanoparticles. Initially, the $AgNO_3$ solution exhibited a colorless hue, subsequently transforming to a deep brown shade. This change in color is due to the reduction of Ag^+ ions to Ag^0 during the transformation to silver nanoparticles and to the excitation of SPR [21]. Comparable results were found with *Lavandula stoechas* [27], and *Lavandula angustifolia* [28]. The efficacy of the Ag-NPs phyto-synthesis pathway was evaluated using a UV–visible spectrophotometer, revealing a peak absorbance at 440 nm for the biosynthesized nanoparticles. The presence of a single, strong, and broad SPR peak indicated a polydispersity characteristic of the Ag-NPs [29]. Our results are in agreement with those of Hasanin et al. who reported a SPR band at 440 nm for silver nanoparticles synthesized using 0.5 mL of *Lavandula coronopifolia* extract. This biosynthesis approach presents a viable and stable method, as plants inherently possess biochemical substances that act as reducing or stabilizing agents, obviating the need for external chemicals [30].

To determine the crystallinity of green produced Ag-LM-NPs, X-ray diffraction analysis was conducted after 24 h of reaction. The XRD pattern exhibited a crystalline phase of silver, identified based on the Crystallography Open Database (COD) with the identification number

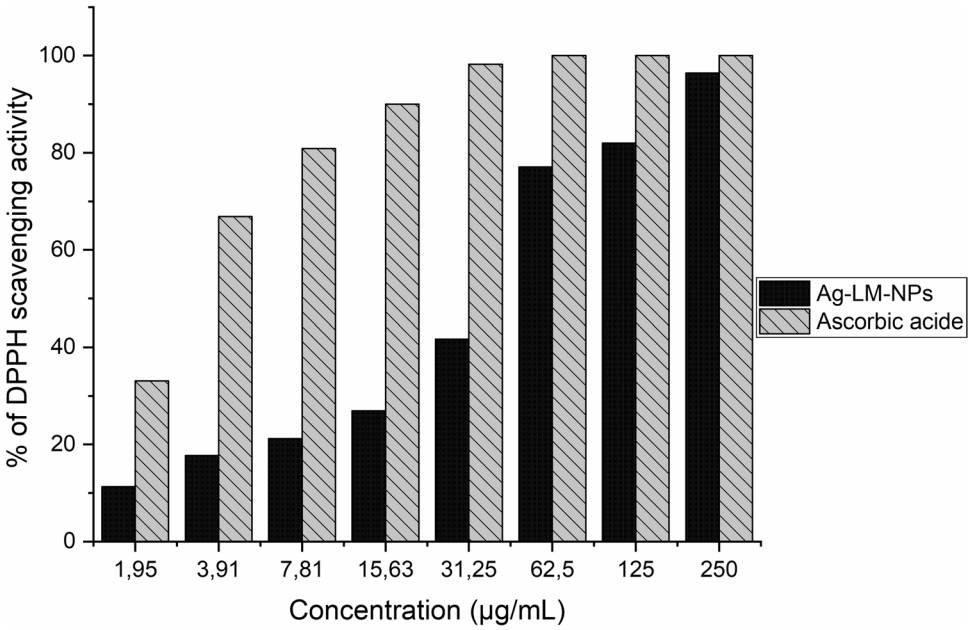

Fig. 5 Percentage of DPPH radical scavenging activity assessed at different concentrations of ascorbic acid and silver nanoparticles synthesized from *L. mairei* extract, revealing that silver nanoparticles exhibit scavenging percentages comparable to those of ascorbic acid, highlighting their antioxidant efficacy

of 9012431[31]. Additional peaks observed in the XRD pattern might be attributed to the presence of organic compounds involved in stabilizing Ag-NPs or impurities in the synthesized nanoparticles.

Nowadays, SEM is employed in many domains, including biological and medical sciences, as well as materials science, physics, and chemistry. Due to its high resolution, SEM is one of the most efficient and complete techniques for analyzing and examining microstructures of materials at the micrometer or nanometer scale [32]. Numerous studies have utilized SEM to investigate the shape and size of silver nanoparticles [16, 18, 21]. In the present study, SEM images of silver nanoparticles synthesized from *L. mairei* revealed their spherical and reasonably uniform shape. This observation confirms that the concentration of *L. mairei* extract was adequate to reduce silver nitrate to its nanoform. The average particle size ranged from 40 to 70 nm, slightly larger than Ag-NPs produced by *Lavandula stoechas* [27], and *Lavandula angustifolia* [28], which measured 20–50 nm and 18 nm, respectively. Al Sufyani et al. [15] reported that *Lavandula dentata* leaf extracts yielded Ag-NPs larger than those found in the present study, which was 284.5 nm. The variation in particle size could be attributed to different synthesis conditions, such as pH, temperature [33], and concentration of the plant extract [29].

The purity and elemental composition of the nanoparticles were investigated by EDS and elemental mapping. In this study, EDS analysis was carried out for Ag-NPs biosynthesized using *L. mairei*, which confirmed the detection of elemental silver. The observed optical absorption band peak at 3 keV aligns with the absorption characteristics typically exhibited by silver nanocrystallites [19]. When compared to O, which accounted for the least weight, carbon (C) and chlorine (Cl) made up a larger percentage. Additionally, the specific crystal structure formed during synthesis significantly influences the stability of Ag-NPs [34].

To investigate the function of different functional groups of *L. mairei*'s phytoconstituents responsible for the production and stabilization of Ag-NPs, FTIR analysis was conducted. The results in Fig. 4 support the existence of certain functional groups active on the surface of Ag-NPs involved in the *L. mairei* extract. The absorption band at 1651 cm^{-1} is attributed to stretching vibrations of C = C and C = N double bonds [35]. The stretching at 3415 cm^{-1} was due to presence of the –OH groups functional [36]. These FTIR spectra suggest that the C = C and –OH groups are adsorbed on the nanoparticle surface, contributing to the stabilization of the synthesized silver nanoparticles. This result can be attributed to the presence of flavonoids, proteins, or phenolic compounds within the plant extract [33].

In the present work, *L. mairei* was selected for Ag-NPs synthesis due to its therapeutic properties. Several studies have confirmed that *L. mairei* was an effective antibacterial agent against pathogenic organisms [6, 22]. Additionally, numerous research papers have demonstrated the effectiveness of silver nanoparticles against antibiotic-resistant bacteria [11, 12]. These reports collectively highlight the excellent antibacterial activity exhibited by both silver nanoparticles and *L. mairei* plant extract. Therefore, the synthesis of silver nanoparticles from *L. mairei* will be a highly effective antibacterial agent. Ag-NPs synthesized by *L. mairei* were utilized in this study to develop new

antibacterial agents against several MDR strains. These synthesized nanoparticles showed high antibacterial activity against all tested MDR *A. baumannii* strains, as indicated by their remarkably low MIC values ranging from 78 ± 0.00 to 312 ± 0.00 µg/mL. However, it is important to acknowledge the limitation of our study regarding the amplicon lengths obtained for 16S rRNA sequencing, which average around 400 base pairs (bp). These amplicons fall notably short of the recommended minimum length of 1000 nucleotides (nt) necessary for robust taxonomic assignment and phylogenetic analysis. This shortfall in sequence length compromises the resolution and fidelity of genetic information crucial for species-level identification. Acknowledging these limitations is pivotal for a nuanced interpretation of findings, recognizing the inherent constraints imposed by data quality [37]. According to literature, there have been no published studies on the antibacterial activity of silver nanoparticles synthesized from *L. mairei* against clinical MDR isolates. Our results are in agreement with previous studies as reported by Wintachai et al. who showed antibacterial activity of Ag-NPs synthesized using *Eucalyptus citriodora* ethanol leaf extract against clinically MDR *A. baumannii* [38]. Similarly, silver nanoparticles biosynthesized by filamentous algae extract showed high antibacterial activity against nosocomial pathogenic *A. baumannii* with MICs of 80 to 640 µg/mL [39]. However, a study by Khan et al. revealed that *Pinus wallichiana*-produced Ag-NPs must be used at relatively high concentrations, MIC approximately 2360 µg/mL, in order to effectively inhibit the growth of *A. baumannii* [40]. Moreover, Shah et al. evaluated the antibacterial activity of chemical Ag-NPs against carbapenem-resistant *A. baumannii*, with MICs in the range of 7000–25000 µg/mL [41], confirming the superior efficacy of biologically synthesized Ag-NPs. Alzahrani et al. reported that silver nanoparticles synthesized from *Ziziphus spina-christi* extracts exhibited higher antibacterial activity (MIC = 61.33 µg/mL) compared to gold nanoparticles (MIC = 104 µg/mL) against MDR *A. baumannii*, indicating that Ag-NPs are the most effective in controlling MDR *A. baumannii* [42]. Additionally, these Ag-NPs produced by *L. mairei* demonstrated significant antibacterial activity against ESBL-producing Enterobacteriaceae strains, including *K. pneumoniae*, *E. coli*, and *E. cloacae*, with a MIC range of 78–625 ± 0.00 µg/mL. Similarly, Ag-NPs synthesized by *Rhizopus stolonifer* exhibited potent antibacterial activity against ESBL-producing Enterobacteriaceae strains, *E. coli*, *Proteus sp.,* and *Klebsiella sp.* [43]. Vamanu and co-workers reported that Ag-NPs synthesized from Mushroom extract displayed strong antibacterial activity against *E. coli* ATCC 25922 [44]. In addition, Edhari et al. [45] showed the effect of chemical Ag-NPs against MDR strains of *K. pneumoniae*, revealing a MIC of 4000 µg/mL, which is higher than that found for bio-Ag-NPs produced in our study. Although the exact antibacterial mechanism of silver nanoparticles is not fully elucidated, their primary mode of action involves adherence to and penetration of the bacterial cell wall. Once inside the cell, they exert additional damage by interacting with sulfur- and phosphorus-containing substances, such as DNA, proteins, enzymes, and phosphorus compounds, ultimately leading to cell death [46].

Plants possess a potent antioxidant capacity and their antioxidant ability can be further enhanced by combining them with metal salts. Previous research demonstrated a significant increase in the antioxidant activity of plants when combined with metals, such as copper, zinc, silver, gold, iron, and titanium [47]. In the present study, the antioxidant activity of green-synthesized Ag-NPs was initially evaluated using the DPPH test. This test is considered as a simple, most effective, and widely used method to evaluate antioxidant activity in vitro [17]. Silver nanoparticles synthesized in the present study from *L. mairei* extracts showed a very interesting DPPH radical scavenging capacity. The level of inhibition observed is higher than that found in another study performed by Mahmoudi et al. which they found that Ag-NPs synthesized by *Lavandula stoechas* have a percentage of inhibition of 60% at 15,000 µg /mL [27]. Furthermore, Ödemiş et al. [48] succeeded in reducing 50% of DPPH by a concentration of 200 µg/mL of Ag-NPs synthesized using *Lavandula angustifolia.* The antioxidant potential of Ag-LM-NPs was also analyzed by FRAP assay. This assay showed that Ag-LM-NPs were able to reduce the reaction system. As a result, it facilitated the reduction of Fe^{+3} to Fe^{+2}, resulting in the formation of the blue complex and indicating great reducing power. As the concentration levels increased, the reducing power also escalated, which aligns with the findings reported by Aruna and Sr. regarding silver nanoparticles biosynthesized from *Costus pictus* [49]. Additionally, silver nanoparticle produced by *Origanum onites* extract showed a significant antioxidant potential [13]. The antioxidant capacity of Ag-NPs could be related to the ability of the phyto-molecules, such as polyphenols, present on the nanoparticles to provide hydrogen or electrons. As a result, the silver nanoparticles produced from *L. mairei* showed strong antioxidant activity. They may therefore be applied to the food and pharmaceutical industries.

Conclusion

In recent years, nanotechnology has developed as a promising research discipline, due to its numerous uses in the healthcare, environmental, and industries sectors. In the present study, stable and biologically active silver nanoparticles were successfully synthesized using the aqueous extract of *L. mairei* for the first time. The biosynthesized Ag-NPs were characterized by UV–visible

spectroscopy, FTIR, XRD, SEM, and EDX analyses. These nanoparticles showed high antibacterial activity against the tested MDR bacteria along with significant antioxidant properties. The technique used in this work to produce Ag-NPs is quick, practical from an economic standpoint, harmless to the environment, and ideal for mass manufacturing. This discovery opens up new avenues for exploring the potential of biologically synthesized nanostructured products for multifaceted applications in healthcare. However, further investigations are required to elucidate other biological activities and the underlying mechanisms of action associated with these nanoparticles.

Author Contribution Soufiane El megdar contributed to writing of the original draft, writing, reviewing, & editing of the manuscript, methodology, and results analysis; Lahbib Fayzi contributed to methodology and plant extraction; Raja Elkheloui contributed to methodology and writing, reviewing, & editing of the manuscript; Asma Laktib contributed to isolation and identification of bacterial strains; Mohamed Bourouache contributed to statistical analysis; Abdellah El boulani contributed to results analysis; Hicham Abou oualid contributed to visualization and correction; Khalil Cherifi contributed to review and correction of paper; Fouad Msanda contributed to collection and identification of plant; Hassi Mohamed contributed to review and correction of paper; Rachida Mimouni contributed to writing, reviewing, & editing of the manuscript, methodology, and results analysis. Fatima Hamadi contributed to writing of the original draft, writing, reviewing, & editing of the manuscript, methodology, and results analysis.

Funding This work was supported by the Moroccan National center of scientific and technical research (VPMA3; n°: 576/2021), the National Agency for Medicinal and Aromatic Plants, and the Ministry of National Education, Vocational Training, Higher Education, and Scientific Research.

Code Availability Not applicable.

Declarations

Conflict of interest The authors have no conflicts of interest.

Ethical Approval Not applicable.

Consent to Participate Not applicable.

Consent for Publication Not applicable.

References

1. Goossens H, Ferech M, Stichele RV, Elseviers M (2005) Outpatient antibiotic use in Europe and association with resistance: a cross-national database study. The Lancet 365:579–587. https://doi.org/10.1016/S0140-6736(05)17907-0
2. Alexander HK, MacLean RC (2020) Stochastic bacterial population dynamics restrict the establishment of antibiotic resistance from single cells. Proc Natl Acad Sci 117:19455–19464. https://doi.org/10.1073/pnas.1919672117
3. Ansari MA, Khan HM, Khan AA et al (2014) Antibiofilm efficacy of silver nanoparticles against biofilm of extended spectrum β-lactamase isolates of Escherichia coli and Klebsiella pneumoniae. Appl Nanosci 4:859–868. https://doi.org/10.1007/s13204-013-0266-1
4. Elkheloui R, Laktib A, Mimouni R et al (2020) Acinetobacter baumannii Biofilm: Intervening Factors, Persistence, Drug Resistance and Strategies of Treatment. Mediterranean J Infection, Microbes and Antimicrobials. https://doi.org/10.4274/mjima.galenos.2020.2020.7
5. Haque A, Yoshizumi A, Saga T et al (2014) ESBL-producing enterobacteriaceae in environmental water in Dhaka, Bangladesh. J Infect Chemother 20:735–737. https://doi.org/10.1016/j.jiac.2014.07.003
6. Laktib A, Nayme K, Hamdaoui AE et al (2022) Antibacterial activity of Lavandula mairei Humbert essential oil against carbapenem- resistant Acinetobacter baumannii. Mediterranean J Infection, Microbes and Antimicrobials. https://doi.org/10.4274/mjima.galenos.2021.2021.3
7. Romero L, López L, Rodríguez-Baño J et al (2005) Long-term study of the frequency of escherichia coli and klebsiella pneumoniae isolates producing extended-spectrum β-lactamases. Clin Microbiol Infect 11:625–631. https://doi.org/10.1111/j.1469-0691.2005.01194.x
8. Laktib A, Hassi M, Hamadi F et al (2018) Identification and antibiotic resistance of nosocomial bacteria isolated from the hospital environment of two intensive care units. Moroccan J Biol 15:24–41
9. Zarrilli R, Giannouli M, Tomasone F et al (2009) Carbapenem resistance in Acinetobacter baumannii: the molecular epidemic features of an emerging problem in health care facilities. J Infect Dev Ctries 3:335–341. https://doi.org/10.3855/jidc.240
10. Tiwari V, Kapil A, Moganty RR (2012) Carbapenem-hydrolyzing oxacillinase in high resistant strains of acinetobacter baumannii isolated from India. Microb Pathog 53:81–86. https://doi.org/10.1016/j.micpath.2012.05.004
11. Gordon O, Vig Slenters T, Brunetto PS et al (2010) Silver coordination polymers for prevention of implant infection : thiol interaction, impact on respiratory chain enzymes, and hydroxyl radical induction. Antimicrob Agents Chemother 54:4208–4218. https://doi.org/10.1128/AAC.01830-09
12. Lara HH, Ayala-Núñez NV, Ixtepan Turrent LD, Rodríguez PC (2010) Bactericidal effect of silver nanoparticles against multidrug-resistant bacteria. World J Microbiol Biotechnol 26:615–621. https://doi.org/10.1007/s11274-009-0211-3
13. Genc N (2021) Biosynthesis of silver nanoparticles using *Origanum onites* extract and investigation of their antioxidant activity. Part Sci Technol 39:562–568. https://doi.org/10.1080/02726351.2020.1786868
14. Mickymaray, (2019) One-step synthesis of silver nanoparticles using saudi arabian desert seasonal plant sisymbrium irio and antibacterial activity against multidrug-resistant bacterial strains. Biomolecules 9:662. https://doi.org/10.3390/biom9110662
15. Al Sufyani NM, Hussien NA, Hawsawi YM (2019) Characterization and anticancer potential of silver nanoparticles biosynthesized from *Olea chrysophylla* and *Lavandula dentata* leaf extracts on hct116 colon cancer cells. J Nanomater 2019:1–9. https://doi.org/10.1155/2019/7361695
16. Ramzan M, Karobari MI, Heboyan A et al (2022) Synthesis of silver nanoparticles from extracts of wild ginger (*Zingiber zerumbet*) with antibacterial activity against selective multidrug resistant oral bacteria. Molecules 27:2007. https://doi.org/10.3390/molecules27062007
17. Konappa N, Udayashankar AC, Dhamodaran N et al (2021) Ameliorated antibacterial and antioxidant properties by trichoderma harzianum mediated green synthesis of silver

nanoparticles. Biomolecules 11:535. https://doi.org/10.3390/biom11040535
18. Huq MdA, Ashrafudoulla Md, Rahman MM et al (2022) Green synthesis and potential antibacterial applications of bioactive silver nanoparticles: a review. Polymers 14:742. https://doi.org/10.3390/polym14040742
19. Bindhu MR, Umadevi M (2015) Antibacterial and catalytic activities of green synthesized silver nanoparticles. Spectrochim Acta Part A Mol Biomol Spectrosc 135:373–378. https://doi.org/10.1016/j.saa.2014.07.045
20. Baran A, Baran MF, Keskin C et al (2021) Ecofriendly/Rapid synthesis of silver nanoparticles using extract of waste parts of artichoke (Cynara scolymus L.) and evaluation of their cytotoxic and antibacterial activities. J Nanomater 2021:1–10. https://doi.org/10.1155/2021/2270472
21. Ahmed MJ, Murtaza G, Rashid F, Iqbal J (2019) Eco-friendly green synthesis of silver nanoparticles and their potential applications as antioxidant and anticancer agents. Drug Dev Ind Pharm 45:1682–1694. https://doi.org/10.1080/03639045.2019.1656224
22. El Hamdaoui A, Msanda F, Boubaker H et al (2018) Essential oil composition, antioxidant and antibacterial activities of wild and cultivated Lavandula mairei Humbert. Biochem Syst Ecol 76:1–7. https://doi.org/10.1016/j.bse.2017.11.004
23. Qais FA, Shafiq A, Ahmad I et al (2020) Green synthesis of silver nanoparticles using Carum copticum: assessment of its quorum sensing and biofilm inhibitory potential against gram negative bacterial pathogens. Microb Pathog 144:104172. https://doi.org/10.1016/j.micpath.2020.104172
24. Ganesan P, Kumar CS, Bhaskar N (2008) Antioxidant properties of methanol extract and its solvent fractions obtained from selected Indian red seaweeds. Biores Technol 99:2717–2723. https://doi.org/10.1016/j.biortech.2007.07.005
25. Duan X-J, Zhang W-W, Li X-M, Wang B-G (2006) Evaluation of antioxidant property of extract and fractions obtained from a red alga, Polysiphonia urceolata. Food Chem 95:37–43. https://doi.org/10.1016/j.foodchem.2004.12.015
26. Chandini SK, Ganesan P, Bhaskar N (2008) In vitro antioxidant activities of three selected brown seaweeds of India. Food Chem 107:707–713. https://doi.org/10.1016/j.foodchem.2007.08.081
27. Mahmoudi R, Aghaei S, Salehpour Z et al (2020) Antibacterial and antioxidant properties of phyto-synthesized silver nanoparticles using *Lavandula stoechas* extract. Appl Organometallic Chem. https://doi.org/10.1002/aoc.5394
28. Villalpando M, Gómez-Hurtado MA, Rosas G, Saavedra-Molina A (2022) Ag nanoparticles synthesized using Lavandula angustifolia and their cytotoxic evaluation in yeast. Mater Today Commun 31:103633. https://doi.org/10.1016/j.mtcomm.2022.103633
29. Nayak S, Bhat MP, Udayashankar AC et al (2020) Biosynthesis and characterization of *Dillenia indica*-mediated silver nanoparticles and their biological activity. Appl Organometallic Chem. https://doi.org/10.1002/aoc.5567
30. Hasanin MS, Emam M, Soliman MMH et al (2022) Green silver nanoparticles based on Lavandula coronopifolia aerial parts extract against mycotic mastitis in cattle. Biocatal Agric Biotechnol 42:102350. https://doi.org/10.1016/j.bcab.2022.102350
31. Diantoro M, Suprayogi T, Sa'adah U, et al (2018) Modification of Electrical Properties of Silver Nanoparticle. IntechOpen J. https://doi.org/10.5772/intechopen.75682
32. Kong Y, Paray BA, Al-Sadoon MK, Fahad Albeshr M (2021) Novel green synthesis, chemical characterization, toxicity, colorectal carcinoma, antioxidant, anti-diabetic, and anticholinergic properties of silver nanoparticles: a chemopharmacological study. Arab J Chem 14:103193. https://doi.org/10.1016/j.arabjc.2021.103193
33. Mohammadi SS, Ghasemi N, Ramezani M, Khaghan S (2021) Biosynthesis of silver nanoparticles using the *Falcaria Vulgaris* (*Alisma Plantago-Aquatica* L.) extract and optimum synthesis. Chem Methodol. https://doi.org/10.22034/chemm.2021.130725
34. Jassal V, Shanker U, Gahlot S et al (2016) Sapindus mukorossi mediated green synthesis of some manganese oxide nanoparticles interaction with aromatic amines. Appl Phys A 122:1–12. https://doi.org/10.1007/s00339-016-9777-4
35. Mochalov K, Solovyeva D, Chistyakov A et al (2016) Silver nanoparticles strongly affect the properties of bacteriorhodopsin, a photosensitive protein of halobacterium salinarium purple membranes. Mater Today: Procee 3:502–506. https://doi.org/10.1016/j.matpr.2016.01.081
36. Popescu C-M, Vasile C, Popescu M-C et al (2006) Analytical methods for lignin characterizatioN. II spectroscopic studies. Cellulose Chem Technol 40:597–622
37. Stackebrandt E, Mondotte JA, Fazio LL et al (2021) Authors need to be prudent when assigning names to microbial isolates. Curr Microbiol 78:4005–4008. https://doi.org/10.1007/s00284-021-02678-4
38. Wintachai P, Paosen S, Yupanqui CT, Voravuthikunchai SP (2019) Silver nanoparticles synthesized with Eucalyptus critriodora ethanol leaf extract stimulate antibacterial activity against clinically multidrug-resistant Acinetobacter baumannii isolated from pneumonia patients. Microb Pathog 126:245–257. https://doi.org/10.1016/j.micpath.2018.11.018
39. Danaei M, Motaghi MM, Naghmachi M et al (2021) Green synthesis of silver nanoparticles (AgNPs) by filamentous algae extract: comprehensive evaluation of antimicrobial and anti-biofilm effects against nosocomial pathogens. Biologia 76:3057–3069. https://doi.org/10.1007/s11756-021-00808-8
40. Khan N, Khan I, Nadhman A et al (2020) *Pinus wallichiana* -synthesized silver nanoparticles as biomedical agents: in-vitro and in-vivo approach. Green Chem Lett Rev 13:69–82. https://doi.org/10.1080/17518253.2020.1733105
41. Shah AA, Ahmad I, Shafique M et al (2022) Antibacterial activity of silver nanoparticles against carbapenem-resistant Acinetobacter baumannii clinical isolates. Pakistan J Pharm Sci 35:203–208. https://doi.org/10.36721/PJPS.2022.35.1.SUP.203-208.1
42. Alzahrani S, Ali HM, Althubaiti EH, Ahmed MM (2022) Green synthesis of gold nanoparticles, silver nanoparticles and gold-silver alloy nanoparticles using ziziphus spina-christi leaf extracts and antibacterial activity against multidrug-resistant bacteria. Indian J Pharm Sci. https://doi.org/10.36468/pharmaceutical-sciences.spl.490
43. Banu A, Rathod V, Ranganath E (2011) Silver nanoparticle production by *Rhizopus stolonifer* and its antibacterial activity against extended spectrum β-lactamase producing (ESBL) strains of enterobacteriaceae. Mater Res Bull 46:1417–1423. https://doi.org/10.1016/j.materresbull.2011.05.008
44. Vamanu E, Ene M, Biță B et al (2018) In vitro human microbiota response to exposure to silver nanoparticles biosynthesized with mushroom extract. Nutrients 10:607. https://doi.org/10.3390/nu10050607
45. Edhari BA, Mashreghi M, Makhdoumi A, Darroudi M (2021) Antibacterial and antibiofilm efficacy of Ag NPs, Ni NPs and Al2O3 NPs singly and in combination against multidrug-resistant Klebsiella pneumoniae isolates. J Trace Elem Med Biol 68:126840. https://doi.org/10.1016/j.jtemb.2021.126840
46. Singh M, Singh S, Prasad S, Gambhir IS (2008) Nanotechnology in medicine and antibacterial effect of silver nanoparticles. Digest J Nanomater Biostructure 3:115–122
47. Matthäus B (2002) Antioxidant activity of extracts obtained from residues of different oilseeds. J Agric Food Chem 50:3444–3452. https://doi.org/10.1021/jf011440s

48. Odemis O, Ozdemir S, Gonca S, Agirtas MS (2022) Characterization of silver nanoparticles fabricated by green synthesis using urtica dioica and lavandula angustifolia and investigation of antimicrobial and antioxidant. Inorganic and Nano-Metal Chem. https://doi.org/10.1080/24701556.2022.2068584
49. Aruna A, Nandhini SR, Karthikeyan V, Bose P (2014) Comparative in-vitro antioxidant screening of methanolic extract of costus pictus & its silver nanoparticles. Int J Pharm Sci Drug Res 6:334–340